Available online at www.sciencedirect.com
SCIENCE DIRECT®
Biomaterials 26 (2005) 4695–4706
Biomaterials
www.elsevier.com/locate/biomaterials

Viscoelastic and mechanical behavior of recombinant protein elastomers

Karthik Nagapudi[a,f], William T. Brinkman[a], Benjamin S. Thomas[a], Jung O. Park[b,c], Mohan Srinivasarao[b,c], Elizabeth Wright[d], Vince P. Conticello[d], Elliot L. Chaikof[a,e,*]

[a]*Departments of Surgery and Biomedical Engineering, Emory University, Atlanta, GA 30322, USA*
[b]*School of Polymer, Textile and Fiber Engineering, Georgia Institute of Technology, Atlanta, GA 30332, USA*
[c]*School of Chemistry and Biochemistry, Georgia Institute of Technology, Atlanta, GA 30332, USA*
[d]*Department of Chemistry, Emory University, Atlanta, GA 30322, USA*
[e]*School of Chemical and Biomolecular Engineering, Georgia Institute of Technology, Atlanta, GA 30332, USA*
[f]*Merck & Co., Rahway, NJ 07095, USA*

Received 4 August 2004; accepted 18 November 2004

Abstract

Recombinant DNA synthesis was employed to produce elastin–mimetic protein triblock copolymers containing chemically distinct midblocks. These materials displayed a broad range of mechanical and viscoelastic responses ranging from plastic to elastic when examined as hydrated gels and films. These properties could be related in a predictable fashion to polymer block size and structure. While these materials could be easily processed into films and gels, electrospinning proved a feasible strategy for creating protein fibers. All told, the range of properties exhibited by this new class of protein triblock copolymer in combination with their easy processability suggests potential utility in a variety of soft prosthetic and tissue engineering applications.

Keywords: Recombinant protein; Protein polymer; Triblock copolymer; Elastin–mimetic; Mechanical behavior; Viscoelastic properties

1. Introduction

We have recently described a modular convergent biosynthetic strategy that has greatly facilitated the synthesis of high molecular weight recombinant protein triblock copolymers with significant flexibility in the selection and assembly of blocks of diverse size and structure [1,2]. In particular, we have demonstrated that elastin–mimetic BAB protein triblock copolymers can be produced with elastomeric- and plastic-like blocks in a manner analogous to synthetic thermoplastic elastomers.

The design framework for this new class of protein triblock copolymer was derived, in part, from prior studies by Urry et al. [3,4]. Specifically, earlier investigations have noted that the phase behavior and mechanical properties of elastin–mimetic polypeptides depend critically on the identity of the residues within the pentapeptide repeat sequence [(Val/Ile)-Pro-Xaa-Yaa-Gly]. Alterations in the identity of the fourth residue (Yaa) modulates the position of the inverse temperature transition of the polypeptide in aqueous solution in a manner commensurate with the effect of the polarity of the amino acid side chain on polymer–solvent interactions. In particular, increasing the polarity of this residue raises the inverse temperature transition in aqueous solutions, that is, the temperature at which the protein coacervates. In addition, these investigators also observed that in hydrated, radiation crosslinked materials, substitution of an Ala for the consensus Gly

*Corresponding author. 1639 Pierce Drive, Room 5105, Emory University, Atlanta, GA 30322, USA. Tel.: +1 404 727 8413; fax: +1 404 727 3660.
E-mail address: echaiko@emory.edu (E.L. Chaikof).

0142-9612/$ - see front matter © 2005 Elsevier Ltd. All rights reserved.
doi:10.1016/j.biomaterials.2004.11.027

residue in the third (Xaa) position of the repeat sequence changed the mechanical response of the material from elastic to plastic deformation. This effect was attributed to a change from a type II to a type I β turn upon substitution of Pro-Gly with Pro-Ala in the pentapeptide repeat sequence. Accordingly, we have recently expressed two amphiphilic triblock polypeptides that incorporate identical endblocks comprised of a hydrophobic plastic monomer sequence $[(IPAVG)_4(VPAVG)]_n$ separated by a central hydrophilic elastomeric block, containing the monomer sequence $[(VPGVG)_4(VPGEG)]_m$. The repeat sequence of the endblock was chosen such that its inverse temperature transition would reside at or near ambient temperature, which would result in phase separation of the hydrophobic domains from aqueous solution under physiologically relevant conditions (pH 7.4, 37 °C). In turn, the sequence of the central elastomeric repeat unit was chosen so that its transition temperature would be significantly higher than 37 °C ensuring conformational flexibility at this temperature.

In a fashion similar to that observed for synthetic block copolymers, it is anticipated that the capacity to control midblock structure will be an important variable in tuning material properties of protein-based block copolymers [5,6]. In this report, we demonstrate that by varying midblock size and amino acid sequence, virtually crosslinked protein-based materials can be produced that display a wide range of viscoelastic and mechanical properties. Moreover, the potential versatility of these materials is further emphasized by confirming the capacity to process triblock protein polymers into a variety of forms, including films, gels, and fiber networks.

2. Materials and methods

2.1. Synthesis of diblock and triblock protein copolymers

Synthetic methods used to produce the DNA inserts that encode the various block copolymers have been described previously [2,7–9]. Oligonucleotide cassettes encoding the elastic (**A**) and plastic (**B**) repeat units (Table 1) were independently synthesized and inserted into the *Bam*H I/*Hin*D III sites within the polylinkers of pZErO-1 and pZErO-2, respectively. Recombinant clones were isolated after propagation in *Escherichia coli* strain Top10F′ and double-stranded DNA sequence analysis verified the identity of the DNA inserts **A** and **B**. These clones were propagated in *E. coli* strain SCS110 in order to isolate preparative amounts of plasmid DNA. DNA monomers **A** and **B** were liberated from the respective plasmids via restriction digestion with *Bsp*M I and *Sex*A I, respectively. Self-ligation of each DNA cassette afforded a population of concatemers encoding repeats of the plastic and elastic sequences, respectively.

Concatemers derived from DNA monomer **B** were inserted into the *Bsp*M I site of the modified polylinker **C** in plasmid pET-24a. A concatemer encoding sixteen repeats of the plastic sequence was isolated and identified via restriction cleavage with *Kpn* I and *Pst* I. Double-stranded DNA sequence analysis confirmed the integrity of the concatemer within the recombinant plasmid, which was labeled pPC. The concatemer was liberated from pPC via restriction cleavage with *Kpn* I and *Pst* I and purified via preparative agarose gel electrophoresis. Enzymatic ligation was used to join the concatemer cassette to the *Kpn* I/*Pst* I sites within the modified polylinker **D** in plasmid pET-24a. Double stranded DNA sequence analysis confirmed the integrity of the concatemer within the recombinant plasmid, which was labeled pPN. The pair of recombinant plasmids pPN and pPC encoded the *N*-terminal and *C*-terminal domains, respectively, of the diblock polymer **P2** (Scheme 1). Restriction cleavage of each plasmid with *Sex*A I and *Xma* I afforded two fragments, which were separated via preparative agarose gel electrophoresis. Enzymatic ligation of the large fragment of pPN and the small fragment of pPC afforded the recombinant plasmid pP2, which encoded protein **P2** as a single contiguous reading frame within plasmid pET-24a.

Plasmid pP2 was propagated in *E. coli* strain SCS110 and cleaved with restriction endonuclease *Sex*A I. A concatemer encoding the elastin sequence **A** was inserted into the compatible *Sex*A I site of pP2. The recombinant clone was analyzed by restriction digestion with *Kpn* I and *Pst* I, followed by agarose gel electrophoresis. Two clones, pB9 and pC5, were isolated that contained 48 and 30 repeats of the elastic sequence **A**, respectively, and encoded proteins **B9** and **C5**. In a similar manner, two additional triblock plasmids were designed and isolated by inserting concatamers derived from oligonucleotide repeat units **E** and **F** into the compatible *Sex*A I site of plasmid pP2 (Table 1, Scheme 2). These plasmids were designated pPHP and pP2Asn, respectively, which encoded proteins **PHP** and **P2Asn**.

Plasmids pP2, pB9, pC5, pPHP, and pP2Asn were used to transform the *E. coli* expression strain BL21-Gold(DE3). Large-scale fermentation (3 L) was performed at 37 °C in Terrific Broth (TB) medium supplemented with kanamycin (50 μg/mL) [10]. The fermentation cultures were incubated under antibiotic selection for 36–48 h at 37 °C with agitation at 175 rpm in an orbital shaker. Cells were harvested via centrifugation at 4 °C and 4000 *g* for 20 min and the cell pellet was resuspended in lysis buffer (150 mL; 100 mM NaCl, 50 mM Tris-HCl, pH 8.0) and stored at −80 °C. The frozen cells were lysed by three freeze/thaw cycles. Lysozyme (1 mg/mL), protease inhibitor cocktail (5 mL), benzonase (25 U/mL), and $MgCl_2$ (1 mM) were

Table 1
Coding sequences of oligonucleotide cassettes employed for the construction of proteins P2, B9, C5, PHP, and P2Asn

A.											
Val	Pro	Gly	Val	Gly	Val	Pro	Gly	Val	Gly	Val	Pro	Gly
GTA	CCT	GGT	GTT	GGC	GTT	CCG	GGT	GTA	GGT	GTA	CCA	GGC
CAT	GGA	CCA	CAA	CCG	CAA	GGC	CCA	CAT	CCA	CAT	GGT	CCG
Glu	Gly	Val	Pro	Gly	Val	Gly	Val	Pro	Gly	Val	Gly	
GAA	GGT	GTA	CCG	GGT	GTT	GGC	GTA	CCA	GGC	GTT	GGC	
CTT	CCA	CAT	GGC	CCA	CAA	CCG	CAT	GGT	CCG	CAA	CCG	
B.												
Val	Pro	Ala	Val	Gly	Ile	Pro	Ala	Val	Gly	Ile	Pro	Ala
GTA	CCT	GCT	GTT	GGT	ATT	CCG	GCT	GTT	GGT	ATC	CCA	GCT
CAT	GGA	CGA	CAA	CCA	TAA	GGC	CGA	CAA	CCA	TAG	GGA	CGA
Val	Gly	Ile	Pro	Ala	Val	Gly	Ile	Pro	Ala	Val	Gly	
GTT	GGT	ATC	CCA	GCT	GTT	GGC	ATT	CCG	GCT	GTA	GGT	
CAA	CCA	TAG	GGA	GCA	CAA	CCG	TAA	GGC	CGA	CAT	CCA	
C.												
Met	Val	Pro	Gly	Val	Gly	Val	Pro	Gly	Val	Gly	Val	
ATG	GTT	CCG	GGT	GTA	GGT	GTA	CCT	GGT	GTT	GGG	GTA	
TAC	CAA	GGC	CCA	CAT	CCA	CAT	GGA	CCA	CAA	CCC	CAT	
Pro	Gly	Val	Gly	Ile	Pro	Ala	Val	Gly	Stop	Stop		
CCT	GCT	GTT	GGT	ATT	CCT	GCA	GTT	GGC	TGA	TGA		
GGA	CGA	CAA	CCA	TAA	GGA	CGT	CAA	CCG	ACT	ACT		
D.												
Met	Val	Pro	Ala	Val	Gly	Ile	Pro	Ala	Val	Gly	Val	
ATG	GTA	CCT	GCT	GTT	GGT	ATT	CCT	GCA	GTT	GGC	GTT	
TAC	CAT	GGA	CGA	CAA	CCA	TAA	GGA	CGT	CAA	CCG	CAA	
Pro	Gly	Val	Gly	Val	Pro	Gly	Val	Gly	Stop	Stop		
CCG	GGT	GTA	GGT	GTA	CCT	GGT	GTT	GGG	TGA	TGA		
GGC	CCA	CAT	CCA	CAT	GGA	CCA	CAA	CCC	ACT	ACT		
E.												
Ala	Pro	Gly	Gly	Val	Pro	Gly	Gly	Ala	Pro	Gly	Gly	
GCA	CCT	GGT	GGC	GTT	CCG	GGT	GGC	GCT	CCG	GGT	GGT	
CGT	GGA	CCA	CCG	CAA	GGC	CCA	CCG	CGA	GGC	CCA	CCA	
Ala	Pro	Gly	Gly	Val	Pro	Gly	Gly	Ala	Pro	Gly	Gly	
GCT	CCG	GGT	GGT	GTT	CCG	GGT	GGT	GCT	CCT	GGT	GGC	
CGA	CGC	CCA	CCA	CAA	GGC	CCA	CCA	CGA	GGA	CCA	CCG	
Ala	Pro	Gly										
GCA	CCT	GGT										
CGT	GGA	CCA										
F.												
Val	Pro	Gly	Val	Gly	Val	Pro	Asn	Val	Gly	Val	Pro	
GTA	CCT	GGT	GTT	GGC	GTT	CCG	AAC	GTA	GGT	GTA	CCA	
CAT	GGA	CCA	CAA	CCG	CAA	GGC	TTG	CAT	CCA	CAT	GGT	
Asn	Val	Gly	Val	Pro	Asn	Val	Gly	Val	Pro	Asn	Val	
AAT	GTT	GGT	GTA	CCG	AAC	GTT	GGC	GTA	CCA	AAC	GTT	
TTA	CAA	CCA	CAT	GGC	TTG	CAA	CCG	CAT	GGT	TTG	CAA	
Gly	Val	Pro	Gly									
GGC	GTA	CCT	GGT									
CCG	CAT	GGA	CCA									

added to the lysate and the mixture was incubated at 25 °C for 30 min. The cell lysate was incubated for 12 h at 4 °C and was centrifuged at 19,000 *g* for 30 min at 4 °C to pellet the cell debris. The target proteins were purified from the clarified cell lysate by three to five cycles of temperature-induced precipitation (4 °C/37 °C) from 500 mM NaCl solution. Dialysis and lyophilization afforded proteins as fibrous solids. Yields: **P2**, 781 mg/L; **B9**, 418 mg/L; **C5**, 614 mg/L; **PHP**, 158 mg/L; and **P2Asn**, 728 mg/L.

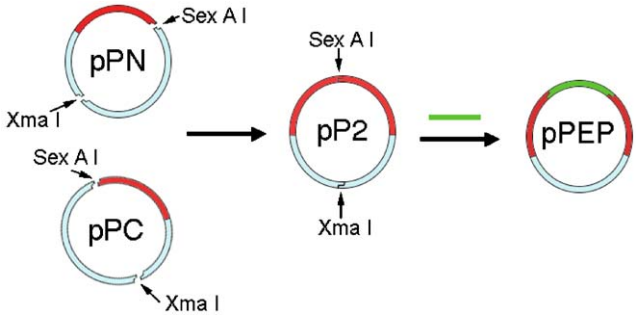

Scheme 1. Biosynthetic route to diblock **P2** and triblock protein copolymers. DNA cassettes encoding plastic repeat units were independently synthesized and inserted into plasmids engineered as N-terminal (pPN) and C-terminal (pPC) blocks. After double digestion with *Sex* AI and *Xma* I, the two cleavage fragments are joined together via enzymatic ligation to afford plasmid p**P2** with a single *Sex* AI restriction site that is located between the plastic domains. After digestion of p**P2** with *Sex* AI, concatemers derived from oligonucleotide monomers A, E, or F were ligated into p**P2** to yield plasmids, generically designated as p**PEP**, encoding triblock protein copolymers with hydrophobic, plastic endblocks and a hydrophilic midblock.

{VPAVG[(IPAVG)$_4$(VPAVG)]$_{16}$IPAVG}-[X]-{VPAVG[(IPAVG)$_4$(VPAVG)]$_{16}$IPAVG}

P2	[X] = VPGVGVPGVG
B9	[X] = VPGVG[(VPGVG)$_2$VPGEG(VPGVG)$_2$]$_{48}$VPGVG
C5	[X] = VPGVG[(VPGVG)$_2$VPGEG(VPGVG)$_2$]$_{30}$VPGVG
PHP	[X] = VPGVG[(APGGVPGGAPGGAPG)$_2$]$_{23}$VPGVG
P2Asn	[X] = VPGVG[VPGVG(VPNVG)$_4$VPG]$_{12}$VPGVG

Scheme 2. Amino-acid sequence of protein-based block copolymers derived from concatemerization of elastin–mimetic peptide sequences **A**, **B**, **E**, and **F**.

2.2. Amino-acid compositional analysis

P2: Obs (calc): Calc. (mol.−%): Ala, 19.7 (19.8); Gly, 20.1 (20.2); Ile, 14.9 (15.7); Pro, 21.6 (20.0); Val, 23.7 (24.3). **B9**: Obs (calc): Ala, 10.8 (8.1); Glx, 2.0 (2.4); Gly, 28.3 (31.9); Ile, 7.0 (6.4); Pro, 22.8 (20.0); Val, 28.2 (31.2). **C5**: Obs (calc): Ala, 11.14 (10.4); Glx, 2.9 (1.9); Gly, 29.62 (29.6); Ile, 9.64 (8.2); Pro, 17.66 (20.0); Val, 29.51 (29.9). **PHP**: Obs (calc): Ala, 19.4 (18.5); Gly, 30.9 (32.1); Ile, 8.66 (9.41); Pro, 20.6 (22.0); Val, 17.0 (18.0). **P2Asn**: Obs (calc): Ala, 14.8 (14.4); Asn, 4.22 (4.21), Gly, 20.7 (21.4); Ile, 11.4 (11.4); Pro, 19.0 (20.0); Val, 27.9 (28.6). **MALDI-TOF mass spectrometry**, Obs. (Calc.): **P2**, 72,016 (72, 116); **B9**, 165,356 (165,564); **C5**, 134,097 (134,438); **PHP**, 112,649 (112,320); **P2Asn**, 100,256 (100,206).

2.3. Rheological analysis of protein block copolymers in water

Rheological data were acquired on an Advanced Rheological Expansion System (ARES) rheometer (Rheometric Scientific Inc., Newcastle, DE) in parallel plate geometry with a plate diameter of 25 mm. Briefly, 25 wt% protein solutions were prepared by adding ultrafiltered, distilled, deionized water (18 MΩ cm, Continental) to the protein at 5 °C and allowing the solution to equilibrate for 72 h. The gap between parallel plates was adjusted to 0.2–0.35 mm. Dynamic mechanical experiments were performed in shear deformation mode to investigate the behavior of viscosity ($\eta*$), storage modulus (G′, elastic property) and loss modulus (G″, viscous property) under appropriate thermal and mechanical conditions. An initial strain amplitude (γ) sweep was performed at 3 and 37 °C at different frequencies to determine the linear viscoelastic range for the protein polymer. With the exception of frequency sweep experiments, a frequency of 1 rad/s was not used because the torque generated was too low.

The temperature of gelation was determined by heating the samples from 3 to 50 °C at a rate of 2 °C/step. After the desired temperature was reached at each step, an additional 30 s was provided to ensure temperature equilibration. The temperature of gelation and viscoelastic properties subsequent to gelation were tested up to 10 thermal cycles and were found to be reproducible. Temperature jump experiments from 3 to 37 °C were also performed to compare the kinetics of gelation between samples.

2.4. Uniaxial tensile measurements

Block copolymer films were cast from 10 wt% solutions of protein polymer in water. Although protein solutions were prepared at 5 °C, solvent evaporation during film formation was performed at 23 °C. After solvent evaporation, films were hydrated in phosphate buffer saline (PBS, pH 7.4, T 23 °C) for 24 h prior to tensile testing. Hydrated film thickness was measured by optical microscopy using a standard image analysis protocol.

A miniature materials tester Minimat 2000 (Rheometric Scientific Inc., Newcastle, DE) was used to determine the mechanical film properties in the tensile deformation mode with a 20 N load cell, a strain rate of 5 mm/min, and a gauge length of 5 mm. Tensile testing was conducted at room temperature and ambient relative humidity. Eight to ten specimens were tested and values for Young's modulus, tensile strength, and elongation to break reported as mean ± standard deviation.

2.5. Formation of fibers by electrospinning of protein solutions

The elastin–mimetic peptide polymer **B9** was spun into fibers using an electrospinning technique, as detailed elsewhere [11,12]. 2, 2, 2 Trifluoroethanol

(TFE) and water were chosen as solvents for electrospining. TFE is a good solvent for both the hydrophobic and hydrophilic blocks of these proteins at room temperature as compared to water which preferentially solvates the hydrophilic midblock. Thus, materials spun from TFE and water have the potential to exhibit different morphologies and mechanical properties. Briefly, protein polymer solutions (10 wt%) were prepared in water or TFE. TFE-based solutions were extruded with the aid of a syringe pump (Harvard Apparatus, Inc.) through a positively charged metal blunt tipped needle (22 G × 1.5 in) at ambient temperature and pressure and at a flow rate of 30–50 μL/min. Fibers were collected on a grounded aluminum plate located 10–15 cm from the needle tip. A high voltage, low current power supply (ES30P/DDPM, Gamma High Voltage Research, Inc.) was used to establish an electric potential gradient of 18 kV. In the case of water-based systems, spinning was performed at 5 °C with the polymer fibers emerging into a heated box at ambient pressure and 23 °C. The grounded aluminum plate was located inside the heated box. Such an arrangement was necessary since the aqueous polymer solutions exhibit gel points between 8 and 15 °C.

2.6. Scanning electron microscopy of protein fibers

A Hitachi S800 FEG scanning electron microscope was used and operated at 10 kV. High-definition topographic images at low (1000 ×) and medium (30,000 ×) magnifications were digitally recorded with very short dwell times to minimize beam-induced damage. Fiber samples were deposited onto silicon chips for examination by scanning electron microscopy (SEM). The silicon chips were subsequently mounted onto aluminum specimen stubs by means of double-sided carbon tape, and coated with a gold film using a Denton DV-602 Turbo Magnetron Sputter System.

3. Results and discussion

3.1. Synthesis of diblock and triblock protein copolymers

The emergence of genetic engineering of synthetic polypeptides has recently enabled the preparation of multiblock protein copolymers composed of complex peptide sequences in which individual blocks may have different mechanical, chemical, or biological properties [13]. For example, Cappello et al. [14] have produced a series of protein polymers ranging up to 1000 amino acids in size (~85 kDa) that contain both silk- and elastin–mimetic sequences. Silk-like regions, which consist of between 12 and 48 alternating alanine and glycine residues are capable of crystallizing to form virtual crosslinks. These blocks are located between elastin–mimetic domains comprised of repeating VPGVG pentapeptides between 40 and 80 amino acids in length. Similarly, Petka et al. [15] have reported the synthesis of a 230 amino acid (22.5 kDa) recombinant protein triblock copolymer that gels in a thermally reversible manner through the association of a single 42 amino-acid leucine zipper region located in flanking endblocks. As these and other studies have illustrated, multiblock recombinant protein polymers can form biphasic materials that exhibit, to varying degrees, properties of the constituent species.

In this report protein triblock copolymers, derived solely from elastin–mimetic polypeptide sequences, were produced with identical endblock sequences of a hydrophobic plastic sequence $[(IPAVG)_4(VPAVG)]_n$ separated by a central hydrophilic elastomeric block of varying amino acid structure. The repeat sequence of the endblocks was chosen such that their inverse temperature transition would reside at or near ambient temperature (~20 °C), which would result in phase separation of the hydrophobic domains from aqueous solution under physiologically relevant conditions (pH 7.4, T 37 °C). In turn, the sequence of the central elastomeric repeat unit was chosen such that its transition temperature was significantly higher than 37 °C yielding a conformational flexible polymer segment at this temperature. It bears comment that inflammatory or allergic reactions have not been reported in response to related elastin protein homopolymers or random copolymers composed of similar peptide sequences, including VPGVG, VPGKG, VPGEG, IPAVG, and VPAVG [16]. In addition, the selected peptide sequences do not appear to be chemotactic to leukocytes, in contrast to other elastin degradation products [17,18].

Five target protein polymers were synthesized. A diblock consisting of flanking plastic endblocks, designated as **P2**, and corresponding triblock copolymers with unique central elastomeric blocks, designated as **B9, C5, PHP, and P2Asn**. Isolated yields ranged from 150 to 800 mg/dL. Amino-acid analysis confirmed the expected composition for all protein polymers and mass spectrometry verified anticipated molar masses of 72 kD for **P2**, 165 kD for **B9**, 134 kD for **C5**, 112 kD for **PHP**, and 100 kD for **P2Asn**.

3.2. Gel points for diblock and triblock protein copolymers

The sol–gel transition for a given polymer solution can be easily detected by measurement of G′ and G″ as a function of temperature or time at fixed frequency. Various methods have been used to determine the gel point in rheological experiments, based on different definitions [19–25]. However, at temperatures significantly above the system T_g, and if the system is

stoichiometrically balanced, G′ and G″ coincide at the gel point [21], independent of the frequency of dynamic deformation imposed. Indeed, rheological measurements for each of these polymers, when dissolved in water, display a G′–G″ crossover, indicating onset of gelation above the inverse transition temperature of the hydrophobic endblock (Figs. 1B–3B). Moreover, all systems investigated were found to undergo physical and reversible gelation, consistent with a stoichiometrically balanced system. Thus, the G′–G″ crossover point was taken as the gel point, which ranged from 8 to 15 °C (Table 2). The capacity of both the midblock and endblocks to coacervate under appropriate conditions was predictable. However, it bears emphasis that the ability of the chosen endblock sequence [$(IPAVG)_4$(V-PAVG)], to form effective *virtual* crosslinking sites and to retain plastic deformation behavior in the absence of chemical or radiation crosslinking had not been previously described. This behavior was further characterized by an analysis of both mechanical and viscoelastic responses.

3.3. Mechanical behavior and viscoelastic properties of protein triblock copolymer films

The strain level above which the viscoelastic response becomes nonlinear is dependent on polymer composition, molecular weight, concentration, temperature, and frequency, among other factors. Therefore, appropriate comparisons between different polymer systems require that rheological behavior be evaluated in the linear viscoelastic region. For example, at 3 °C both **B9** and **P2Asn** showed linear viscoelasticity up to a strain amplitude of 25%, while **PHP** showed strong nonlinearity beyond a strain amplitude of 4%. However, at 37 °C, where all of these block copolymers are in a gel phase, the viscosities and storage moduli were strain independent within the experimental range. Thus, a strain of 25% was selected to examine the rheological behavior of aqueous solutions of **B9** and **P2Asn** at 3 °C, as lower strains did not generate enough torque, while a strain of 5% was applied in all other experiments. A 2.5% strain level was used for all property measurements for aqueous solutions of **PHP**.

Detailed investigations of the viscoelastic properties of these proteins in water are reported in Figs. 1–4 and critical parameters are summarized in Table 2. At 3 °C, the viscosities of these protein solutions are very low, but the moduli reveal rheological responses near the flow-to-rubbery transition (Figs. 1A–3A). This implies that these systems exhibit appreciable intra- and intermolecular attraction even at low temperature, probably as a result of hydrogen bonding. Upon stepwise heating from 3 to 50 °C, the proteins self-associate via strong intra-and intermolecular physical bonds, which are reversible on cooling. This results in a considerable increase in viscosity and elastic modulus of up to three to four orders of magnitude (Figs. 1B–3B). Gelations were thermoreversible and the rheological responses reproducible upon repeated tests. At 37 °C, all

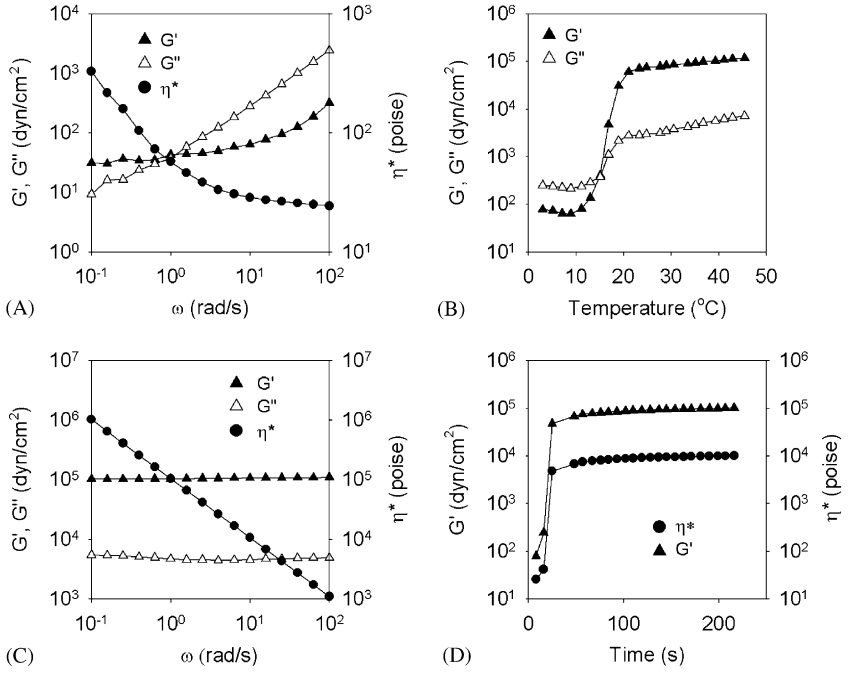

Fig. 1. Rheological behavior of **B9** in water. (A) Dynamic shear storage (G′), loss modulus (G″), and complex viscosity ($\eta*$) are plotted as a function of frequency (γ 25%, 3 °C), (B) G′ and G″ as a function of temperature (γ 5%, ω 10 rad/s), (C) G′, G″, and $\eta*$ as a function of frequency (γ 5%, 37 °C), and (D) G′ and $\eta*$ as a function of time (γ 5%, ω 10 rad/s, 37 °C).

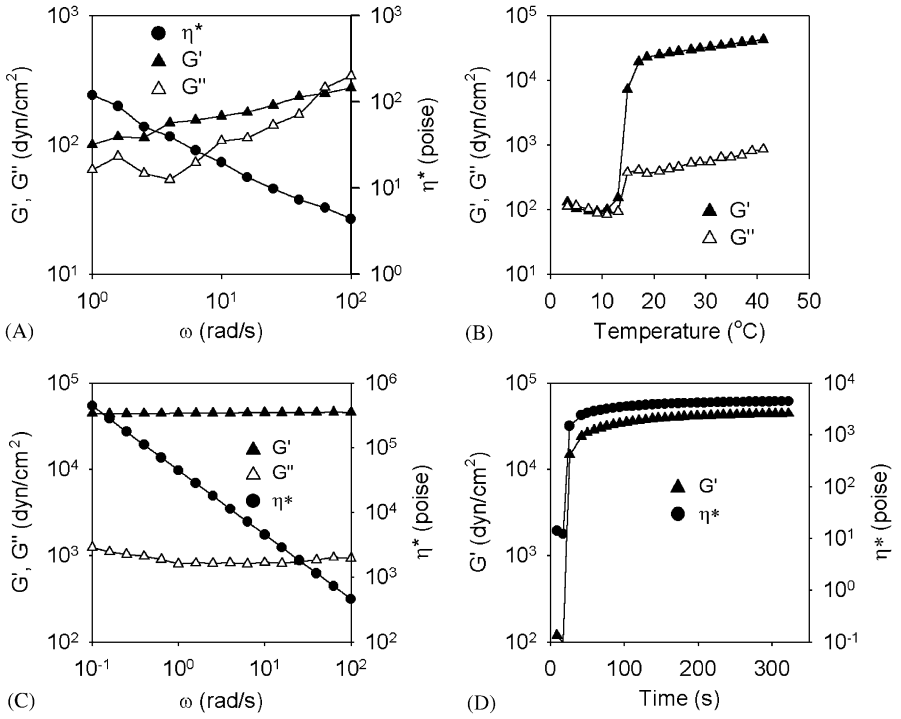

Fig. 2. Rheological behavior of **PHP** in water. (A) Dynamic shear storage (G′), loss modulus (G″), and complex viscosity ($\eta*$) are plotted as a function of frequency (γ 2.5%, 3 °C), (B) G′ and G″ as a function of temperature (γ 2.5%, ω 10 rad/s), (C) G′, G″, and $\eta*$ as a function of frequency (γ 2.5%, 37 °C), and (D) G′ and $\eta*$ as a function of time (γ 2.5%, ω 10 rad/s, 37 °C).

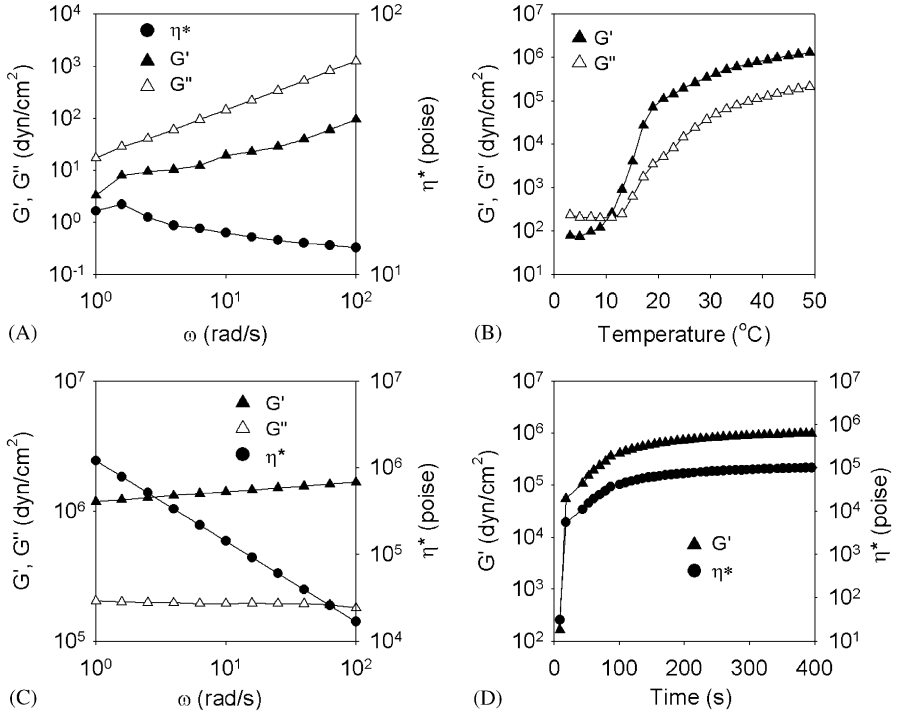

Fig. 3. Rheological behavior of **P2Asn** in water. (A) Dynamic shear storage (G′), loss modulus (G″), and complex viscosity ($\eta*$) are plotted as a function of frequency (γ 25%, 3 °C), (B) G′ and G″ as a function of temperature (γ 5%, ω 10 rad/s), (C) G′, G″, and $\eta*$ as a function of frequency (γ 5%, 37 °C), and (D) G′ and $\eta*$ as a function of time (γ 5%, ω 10 rad/s, 37 °C).

Table 2
Rheological properties of elastin–based protein polymers

Protein	Gel point[a] (°C)	Gel modulus[b] (kPa)	Gel complex viscosity[b] (Poise)	Tan δ[b]
P2	13.2	280	3,000,000	0.1428
C5[c]	14.8	6.5	70,000	0.0128
B9	15.0	10.5	103,000	0.0450
PHP	8.2	4.5	44,500	0.0178
P2Asn	10.4	126	1,200,000	0.1730

[a]G′–G″ crossover temperature measured at $\gamma = 5\%$ (2.5% for PHP), $\omega = 10$ rad/s.
[b]All quantities measured at $\gamma = 5\%$ (2.5% for PHP), $\omega = 1$ rad/s.
[c]Rheological data for C5 was initially published elsewhere [1].

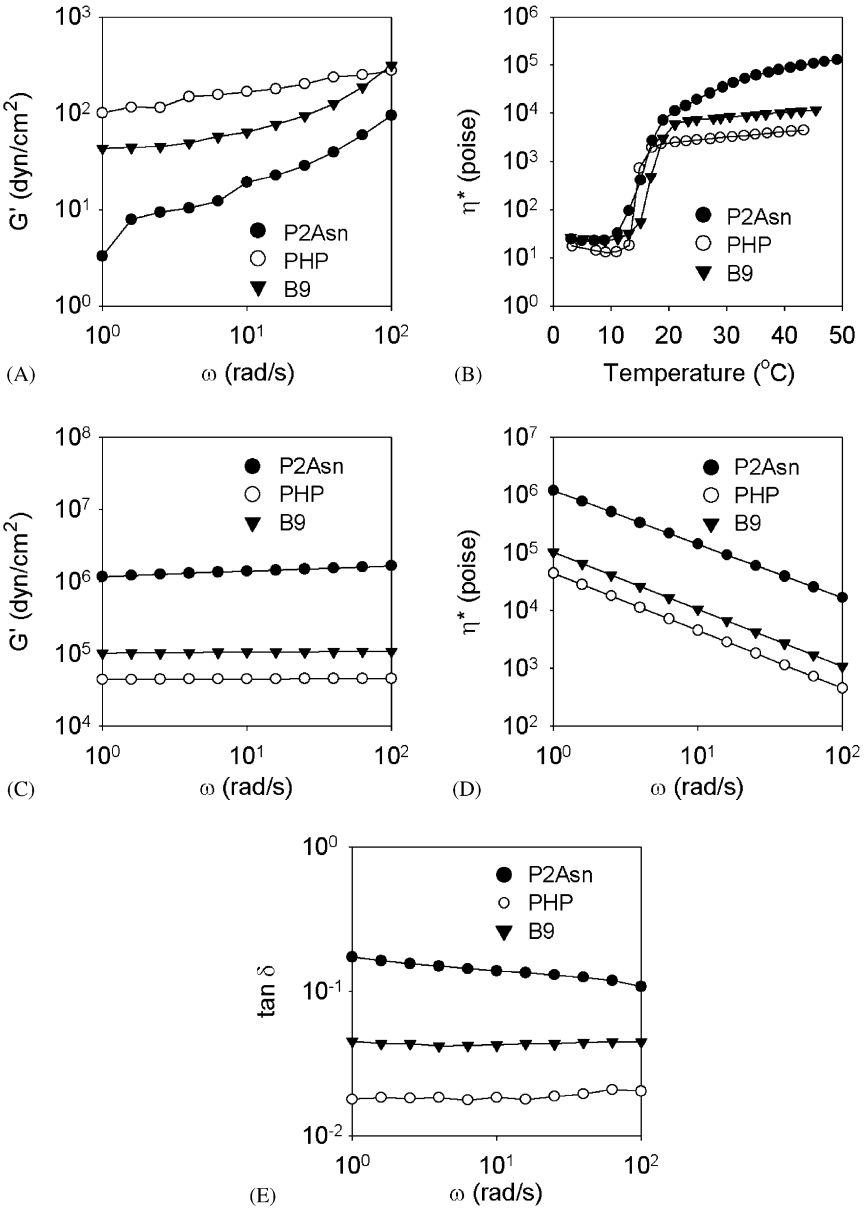

Fig. 4. Comparison of triblock protein polymers **B9**, **P2Asn**, and **PHP**: (A) Shear storage modulus (G′) at 3 °C, (B) Complex viscosity ($\eta*$) as a function of temperature (ω 10 rad/s), (C) Shear storage modulus (G′) at 37 °C, (D) Complex viscosity ($\eta*$) at 37 °C, and (E) Loss tangent (tan δ) at 37 °C.

protein systems demonstrated frequency-dependent viscosities and frequency-independent moduli consistent with the formation of firm gels comprised of strong *virtual* crosslinks (Figs. 1–3C). Temperature jump experiments from 3 to 37 °C revealed that gelation was essentially instantaneous (Figs. 1–3D).

Notably, selected changes in midblock size and amino-acid sequence revealed significant changes in both viscoelastic and mechanical properties. For example, protein polymers **B9** and **C5** were designed with identical midblocks, comprised of $(VPGVG)_4(VPGEG)$ repeat sequences. However, the **B9** midblock was 50% larger in size than that of the **C5** copolymer. Although **B9** exhibited a small but noticeable increase in viscous behavior when compared to **C5**, as represented by an increase in tan δ (Table 2), the rheological properties of both copolymers were quite similar. In contrast, the effect of an increase in midblock size was readily apparent in an analysis of uniaxial stress–strain behavior. Specifically, while little change was observed with respect to Young's modulus or ultimate tensile strength, strain at failure was substantially enhanced by an increase in midblock size (Fig. 5 and Table 3).

The triblock protein **PHP** contains a midblock consisting of APGGVPGGAPGGAPG repeat sequences and its properties are summarized in Fig. 2 and Table 2. Prior studies have suggested that protein polymers based upon repeats of the APGG sequence lack an inverse transition temperature, while those derived from VPGG monomer sequences have a transition temperature of approximately 55 °C [4]. Thus, as a hybrid of both sequences, this midblock was expected to be conformationally flexible at 37 °C. Moreover, in the absence of VPGVG repeats, this block alone would not be expected to display elastomeric properties. Nonetheless, as a consequence of virtual crosslink formation, the triblock protein **PHP** displayed elastomeric responses akin to **C5** and **B9**. In addition, as evident by a significantly lower tan δ, all of these proteins were much more elastomeric than **P2**, which was composed solely of plastic-like endblock sequences· Consistent with these rheological responses, uniaxial testing revealed that **PHP** exhibited a far greater compliance and extensibility than **P2**, albeit with reduced tensile strength. For example, a strain to failure of $128 \pm 33\%$ was observed for **P2**, while values ranging between 500 and 1000% were observed for **PHP**, **C5**, and **B9**. These investigations serve to emphasize that considerable flexibility exists in the choice of midblock structure with retention of elastomer gel properties even in the absence of VPGVG repeat sequences.

The recombinant protein **P2Asn** was designed with repetitive $VPGVG(VPNVG)_4VPG$ sequences in the midblock. Asparagine (N) is a non-charged polar amino acid that was substituted for glycine in the third position of the VPGVG pentapeptide. In a manner analogous to a glycine to alanine substitution, analysis of rheological and mechanical properties revealed plastic-like deformation behavior in which irrecoverable deformation occurred in response to applied stress (Figs. 3 and 5). In this regard, the tan δ measured for **P2** and **P2Asn** was an order of magnitude greater than those values noted for either **B9**, **C5**, or **PHP**. Thus, when compared to other elastin–mimetic copolymers, both **P2** and **P2Asn** are much less elastomeric and display considerable energy losses due to viscous dissipation in response to loading forces. Nonetheless, the tensile strength and modulus of **P2Asn** was significantly lower than **P2**, which demonstrates that the plasticity of **P2** can be moderated by the addition of a *hydrophilic* plastic-like midblock.

A comparative analysis of rheological behavior of these protein triblocks is provided in Fig. 4. At 3 °C, the G′ for aqueous protein solutions demonstrated a rank order of **PHP > B9 > P2Asn** (Fig. 4A). The evolution of $\eta*$ as a function of temperature (Fig. 4B) showed that **P2Asn** exhibited the highest gel viscosity, although the

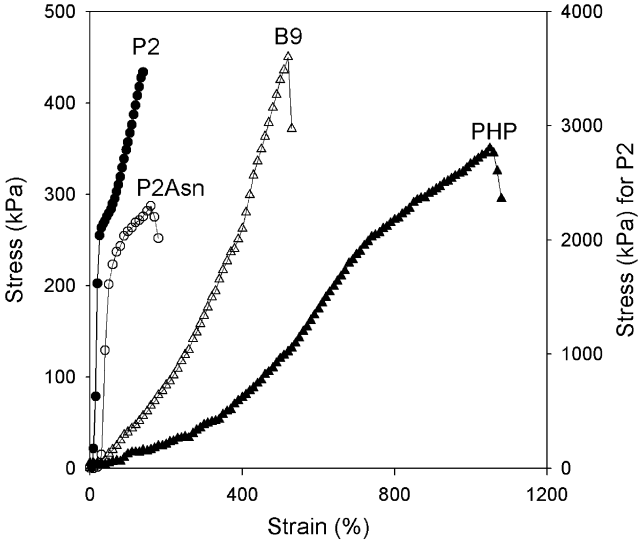

Fig. 5. Uniaxial stress–strain curves for elastin–mimetic protein block copolymers. The right hand y-axis is the stress scale for **P2**.

Table 3
Uniaxial tensile behavior for elastin–based protein polymers

Protein	Young's modulus (MPa)	Tensile strength (MPa)	Strain to failure (%)
P2	16.65 ± 4.55	3.00 ± 0.32	128 ± 33
C5	0.05 ± 0.01	0.96 ± 0.16	822 ± 97
B9	0.03 ± 0.01	0.78 ± 0.28	1084 ± 67
PHP	0.04 ± 0.01	0.31 ± 0.13	505 ± 123
P2Asn	0.97 ± 0.26	0.22 ± 0.04	158 ± 57

onset of a maximum value for $\eta*$ was more gradual than that observed for **B9** or **PHP**. After gelation, frequency-independent G′ (Fig. 4C) and frequency-dependent $\eta*$ (Fig. 4D) were observed consistent with the formation of hard gels. Moreover, comparison of G′ in the gel state for these materials reveals a rank order of **P2Asn > B9 > PHP** that is the reverse order of that observed at 3 °C. An analysis of tan δ, as a measure of gel elasticity, illustrates a rank order of **PHP > B9 > P2∼P2Asn** (Fig. 4E). These results serve to further illustrate that the elastic or plastic nature of protein gels and films can be tailored throughout a wide range of responses by relatively limited changes in chemistry, including midblock size or structure. Of note, gel storage moduli (G′) reported in Table 2 compare with those reported for natural hydrogels, such as hyaluronan [26] and articular cartilage [27].

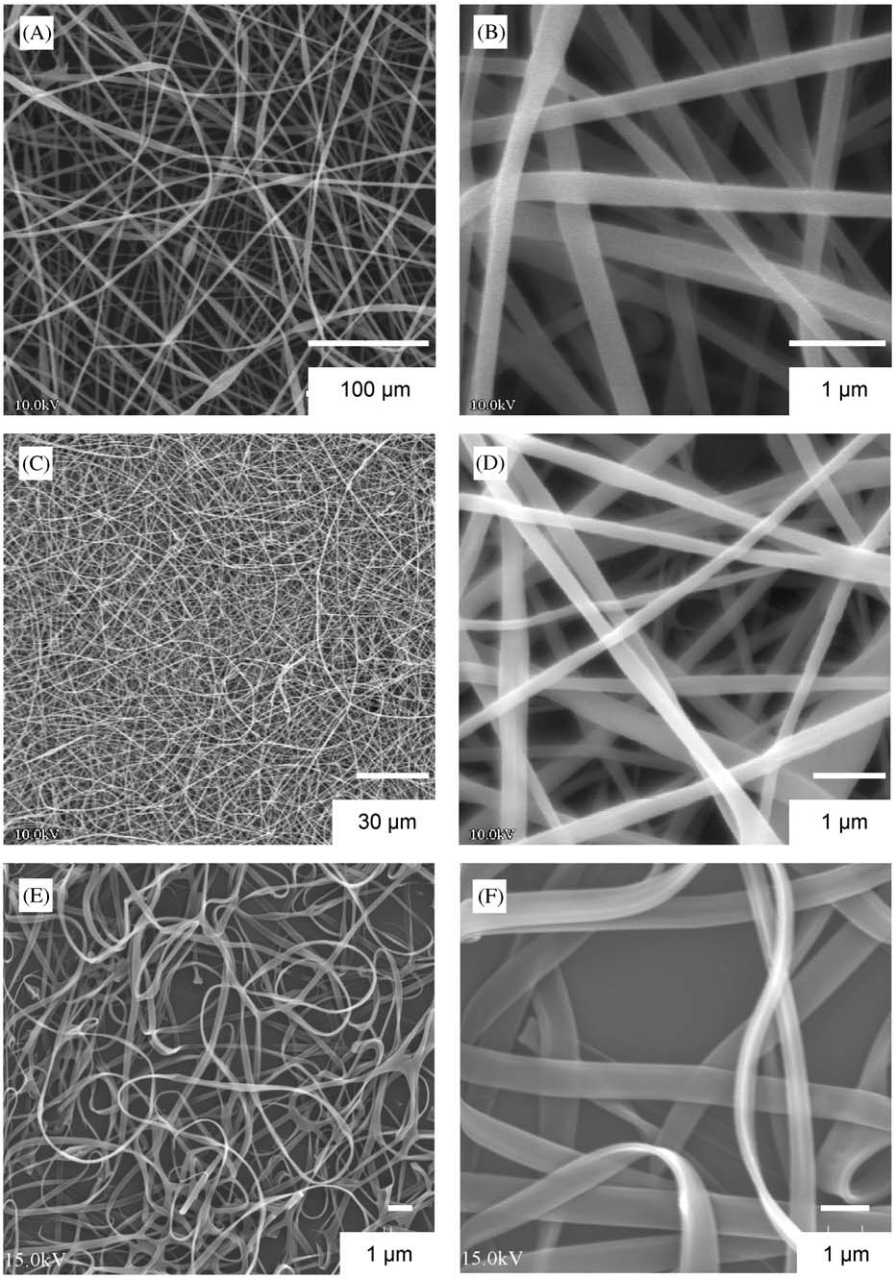

Fig. 6. SEM micrographs of fibers spun from a 10-wt% solution of **P2** in TFE were aquired at a magnification of 2 × (A) and 10,000 × (B). Fibers spun from a 10-wt% solution of **B9** in TFE were examined by SEM at a magnification of 1000 × (C) and 10,000 × (D). Solutions of **P2** and **B9** in TFE generated uniform fibers in the range of 100–400 nm. Fibers spun from a 10-wt% solution of **B9** in water were examined by SEM at a magnification of 1000 × (E) and 5000 × (F). Fibers with diameters ranging between 800 nm and 3 μm were observed.

3.4. High-resolution electron microscopy of protein copolymer fibers

In addition to gels and films, the fabrication of fibers would provide a useful starting point for generating protein scaffolds for tissue engineering applications. In this regard, electrospinning provides a convenient method for producing non-woven fabrics comprised of nanometer scale fibers. When dissolved in TFE, **B9** does not exhibit an inverse transition temperature. Thus, TFE provided a convenient solvent for spinning protein fibers at room temperature. SEM micrographs revealed that uniform nanofibers in the diameter range of 100–400 nm could be produced by room temperature spinning of 10-wt% solutions of **P2** and **B9** in TFE (Fig. 6A–D). Recent studies from our group have revealed that protein polymer behavior can be manipulated by the control of interphase mixing between blocks through the selection of block selective or non-selective solvents [2]. For example, while hydrophobic endblocks undergo selective collapse in water over a temperature range of 8–37 °C, rheological testing demonstrates that this does not occur when protein polymers are dissolved in TFE. As a consequence, mixing of hydrophilic midblocks and hydrophobic endblocks is enhanced for protein gels formed from solutions produced in TFE while limited for those generated from aqueous solution. This has a profound effect on material properties, which is described in detail elsewhere [2]. Thus, in order to fully exploit the available range of mechanical properties that is afforded by these copolymers, fiber spinning was also explored from aqueous solution. Since aqueous solutions of these triblock copolymers gel at room temperature, effective fiber spinning was accomplished by spinning at 5 °C into a heated chamber whose temperature could be controlled from 23 to 60 °C. SEM micrographs of fibers produced from a 10-wt% solution of **B9** in water showed nanofibers with diameters ranging from 800 nm to 3 μm, which were considerably larger than those produced from TFE (Fig. 6E and F). At an identical concentration of **B9**, solutions in TFE displayed a lower viscosity at 23 °C than aqueous protein solutions at 5 °C, which may have contributed to the formation of smaller diameter fibers.

4. Conclusions

Recombinant DNA synthesis was employed to produce viscoelastic protein triblock copolymers containing chemically distinct midblocks. Significantly, in response to selected midblock structures, these materials have the capacity to display a broad range of mechanical responses ranging from plastic to elastic when examined as hydrated gels and films. Moreover, electrospinning proved a feasible strategy for creating protein fibers and fabrics. While TFE facilitated room temperature spinning, temperature-dependent electrospinning allowed use of aqueous solutions, which may allow access to alternate microphase separated structures and, if so desired, would also permit the addition of bioactive compounds that would otherwise be inactivated by organic solvents. The range of properties exhibited by these materials in combination with their easy processability establishes a useful starting point for examining the utility of this new class of protein triblock copolymer in a variety of soft prosthetic and tissue engineering applications.

5. Supporting information

Sequential residue assignments derived from ^{1}H NMR and ^{13}C NMR spectroscopic data measured at 4 °C are available for polypeptides **P2**, **B9**, **C5**, **PHP**, and **P2Asn**.

Acknowledgments

This work was supported by grants from the NIH and NSF.

Appendix A. Supporting information

The online version of this article contains additional supplementary data. Please visit doi:10.1016/j.biomaterials.2004.11.027.

References

[1] Wright ER, McMillan RA, Cooper A, Apkarian RP, Conticello VP. Thermoplastic elastomer hydrogels via self-assembly of an elastin–mimetic triblock polypeptide. Adv Fun Mater 2002; 12:149–54.
[2] Nagapudi K, Brinkman WT, Liesen J, Thomas BS, Wright ER, Haller C, Wu X, Apkarian RP, Conticello VP, Chaikof EL. Protein-based thermoplastic elastomers. Macromolecules 2005;38: 345–54.
[3] Urry DW. Physical chemistry of biological free energy transduction as demonstrated by elastic protein-based polymers. J Phys Chem B 1997;101:11007–28.
[4] Urry DW, Luan C- H, Harris CM, Parker TM. In: McGrath K, Kaplan D, editors. Protein-based materials. Boston: Birkhäuser; 1997. p. 133–78.
[5] Legge NR, Holden G, Schroeder HE, editors. Thermoplastic elastomers. New York: Hanser; 1987.
[6] Spontak RJ, Patel NP. Thermoplastic elastomers: fundamentals and applications. Curr Opin Coll Interface Sci 2000;5:334–41.
[7] Wright ER, Conticello VP. Adv Drug Deliv Rev 2002;54:1057–73.
[8] McMillan RA, Lee TAT, Conticello VP. Rapid assembly of synthetic genes encoding protein polymers. Macromolecules 1999; 32:3643–8.

[9] Lee TAT, Cooper A, Apkarian RP, Conticello VP. Thermoreversible self-assembly of nanoparticles derived from elastin–mimetic polypeptides. Adv Mater 2000;12:1105–10.
[10] Daniell H, Guda C, McPherson DT, Zhang X, Xu J, Urry DW. Hyperexpression of a synthetic protein-based polymer gene. Methods Mol Biol 1997;63:359–71.
[11] Huang L, McMillan RA, Apkarian RP, Pourdeyhimi RP, Conticello VP, Chaikof EL. Generation of synthetic elastin–mimetic small diameter fibers and fiber networks. Macromolecules 2000;33:2989–97.
[12] Nagapudi K, Huang L, McMillan RA, Brinkman W, Conticello VP, Chaikof EL. Photomediated solid-state crosslinking of an elastin–mimetic recombinant protein polymer. Macromolecules 2002;35:1730–7.
[13] Ferrari F, Cappello J. In: McGrath K, Kaplan D, editors. Protein-based materials. Boston: Birkhäuser; 1997. p. 37–60.
[14] Cappello J, Crissman JW, Crissman M, Ferrari FA, Textor G, Wallis O, Whitledge JR, Zhou X, Burman D, Aukerman L, Stedronsky ER. In-situ self-assembling protein polymer gel systems for administration, delivery, and release of drugs. J Control Rel 1998;53:105–17.
[15] Petka WA, Hardin JL, McGrath KP, Wirtz D, Tirrell DA. Reversible hydrogels from self-assembling artificial proteins. Science 1998;281:389–92.
[16] Urry DW, Pattanaik A, Accavitti MA, Luan CX, McPherson DT, Xu J, et al. In: Domb AJ, Kost J, Wiseman DM, editors. Handbook of biodegradable polymers. Amsterdam: Harwood; 1997. p. 367–86.
[17] Hauck M, Seres I, Kiss I, Saulnier J, Mohacsi A, Wallach J, et al. Effects of synthesized elastin peptides on human leukocytes. Biochem Mol Biol Intern 1995;37:45–55.
[18] Fulop Jr T, Jacob MP, Khalil A, Wallach J, Robert L. Biological effects of elastin peptides. Pathol Biol 1998;46:497–506.
[19] Winter HH, Chambon F. Analysis of linear viscoelasticity of a crosslinking polymer at the gel point. J Rheol 1986;30:367–82.
[20] Chiou B- S, English RJ, Khan S. Rheology and photocrosslinking of thiolene polymers. Macromolecules 1996;29:5368–74.
[21] Boey FYC, Qiang W. Determining the gel point of an epoxy-hexaanhydro-4-methylphthalic anhydride (MHHPA) system. J Appl Polym Sci 2000;76:1248–56.
[22] Kelarakis A, Castelletto B, Chaibundit C, Fundin J, Havredaki V, Hamley IW, Boooth C. Rheology and structures of aqueous gels of triblock (oxyethylene/oxybutylene/oxyethylene) copolymers with lengthy oxyethylene blocks. Langmuir 2001;17: 422–4239.
[23] Nair RCP, Ninan KN. Rheological cure characterization of phosphazene-triazine polymers. J Appl Polym Sci 2003;88: 908–14.
[24] de la Caba K, Guerrero P, Eceiza A, Mondragon I. Kinetic and rheological studies of two unsaturated polyester resins cured at different temperatures. Eur Poly J 1997;33:19–23.
[25] Laza JM, Julian CA, Larrauri E, Rodriguez M, Leon LM. Thermal scanning rheometer analysis of curing kinetic of an epoxy resin: 2. an amine as curing agent. Polymer 1999;40: 35–45.
[26] Zhu W, Mow VC, Rosenberg LC, Tang LH. Determination of kinetic changes of aggrecan-hyaluronan interactions in solution from its rheological properties. J Biomechanics 1994;27: 571–9.
[27] Setton LA, Mow VC, Howell D. Mechanical-behavior of articular-cartilage in shear is altered by transection of the anterior cruciate ligament. J Orthop Res 1995;13:473–82.